sEKV Parameter Extraction for the IHP 130nm Process

nMOS (short-channel)

Christian Enz (christian.enz@epfl.ch)

14.02.2026

Table of contents

1 Introduction

In this notebook we will extract the sEKV parameters [1] [2] for a short-channel nMOS transistors from the 130nm bulk CMOS process of IHP [3]. The extraction is done with data generated using the PSP compact model [4] from the PDK of the IHP 130nm process [3] for the typical-typical (t-t) case.

The easiest way to extract the sEKV parameters is to use the python tool developed by H.C. Han and available on GitLab [5]. The tool and the extraction procedure are described in [6]. In this notebook we will detail the extraction procedure and show how the parameters can be extracted manually.

We start by looking at the channel width and length corrections for the drain current and for the capacitances. Then we will extract the sEKV parameter using a direct extraction methodology with the velocity parameter $\lambda_c = 0$. We then will extract the additional parameter λ_c using a direct extraction methodology. Then we will extract all the sEKV parameters by optimization using nonlinear curve fitting.

We also will extract the output conductance due to channel-length modulation (CLM) and the related parameter.

Finally, we will check the white noise model and extract the EKV flicker noise parameters.

The extracted parameters are then all saved in an Excel worksheet.

2 Transistor geometry parameters

2.1 Effective length and width for current

Before we start the extraction we need to account for the geometry dependence. With PSP you can choose between geometry scaling rules or binning rules with parameter $SWGEO$. If $SWGEO = 1$, the scaling rules are chosen. This is the case in the IHP 130nm G2 PDK. The geometrical parameters are defined in Figure 2.1 [4].

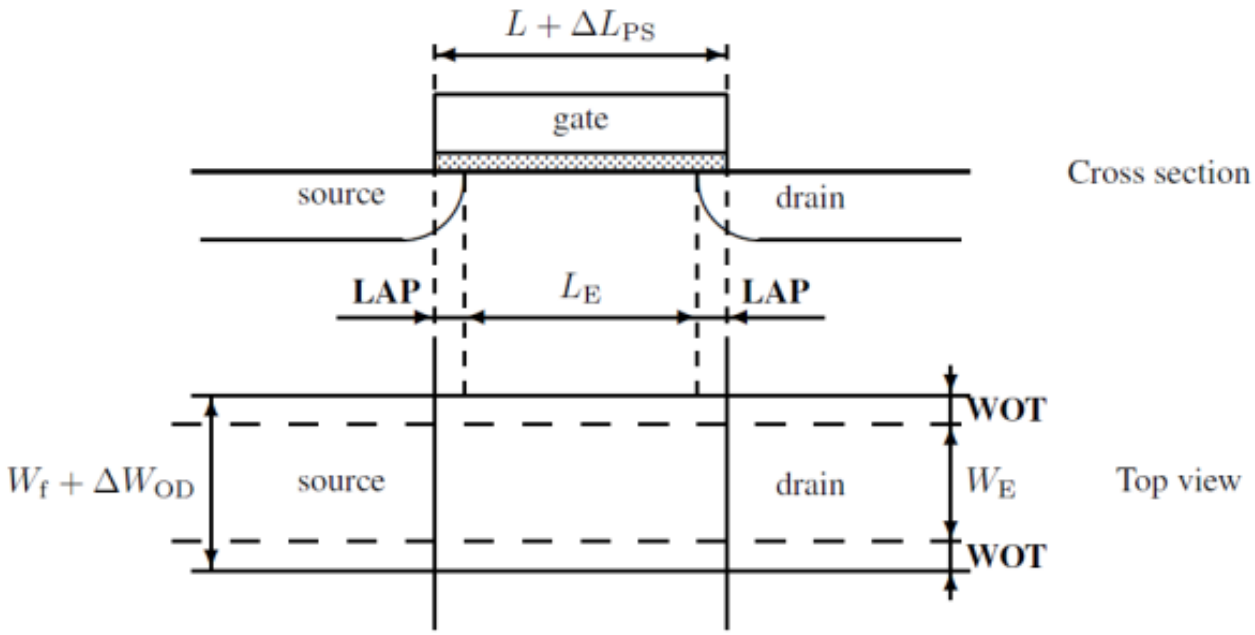

Figure 2.1: Definition of transistor geometrical parameters [4].

The effective length and width are defined as

$$L_{eff} = L - \Delta L, \tag{2.1}$$
$$W_{eff} = W_f - \Delta W, \tag{2.2}$$

where W_f is the width of one finger defined as

$$W_f = \frac{W}{NF}. \tag{2.3}$$

In our case we will assume that the number of fingers $NF = 1$ and hence that $W_f = W$. ΔL and ΔW are given by

$$\Delta L = 2\,LAP - \Delta L_{PS}, \tag{2.4}$$
$$\Delta W = 2\,WOT - \Delta W_{OD}, \tag{2.5}$$

with

$$\Delta L_{PS} = LVARO \cdot \left(1 + LVARL \cdot \frac{L_{EN}}{L}\right) \cdot \left(1 + LVARW \cdot \frac{W_{EN}}{W_f}\right), \tag{2.6}$$

$$\Delta W_{OD} = WVARO \cdot \left(1 + WVARL \cdot \frac{L_{EN}}{L}\right) \cdot \left(1 + WVARW \cdot \frac{W_{EN}}{W_f}\right). \tag{2.7}$$

For nMOS $LVARO = 0$ and $WVARO = 0$ and therefore $\Delta L_{PS} = 0$ and $\Delta W_{OD} = 0$. The length and width reduction then reduce to

$$\Delta L = 2\,LAP, \tag{2.8}$$

$$\Delta W = 2\,WOT. \tag{2.9}$$

The length and width reduction ΔL and ΔW are therefore constant and independent of L and W. Their values are given in Table 2.1.

Table 2.1: Length and width corrections.

Definition	ΔW [nm]	ΔL [nm]	Comment
For current	-20.000	58.846	extracted from PDK

Note that for nMOS ΔW = -20.000 nm is negative wich leads to an effective width that is longer than the drawn width. On the other hand ΔL = 58.846 nm is positive which results in an effective length that is smaller than the drawn length.

The width and length for the selected nMOS transistor are given by $W = 10\ \mu m$ and $L = 130\ nm$ and the effective width and length are given by $W_{eff} = 10.020\ \mu m$ and $L_{eff} = 71\ nm$. They are summarized in Table 2.2.

Table 2.2: Selected transistor width and length.

Type	W [μm]	W_{eff} [μm]	L [nm]	L_{eff} [nm]
nMOS	10	10.020	130	71

3 DC Transfer Characteristic Parameters

3.1 Generating and importing the data

The data used for the sEKV parameters extraction is generated by simulation using ngspice with the PSP CM [4] from the PDK of the IHP 130nm process [3] for the typical-typical (t-t) case. We present the I_D-V_G and G_m-V_G data below.

3.1.1 I_D and G_m versus V_G

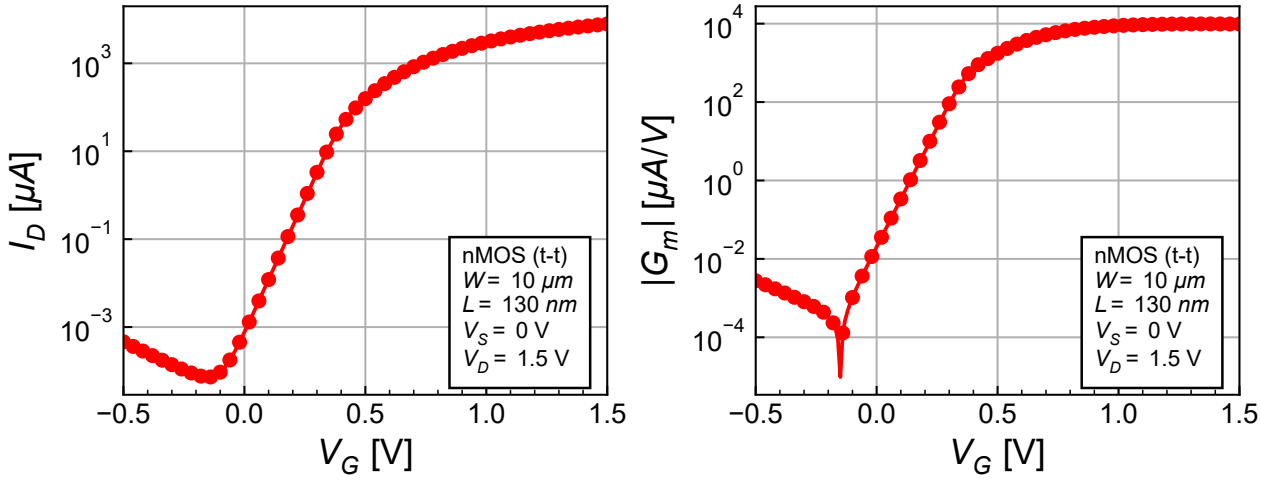

Figure 3.1: Imported I_D-V_G and G_m-V_G.

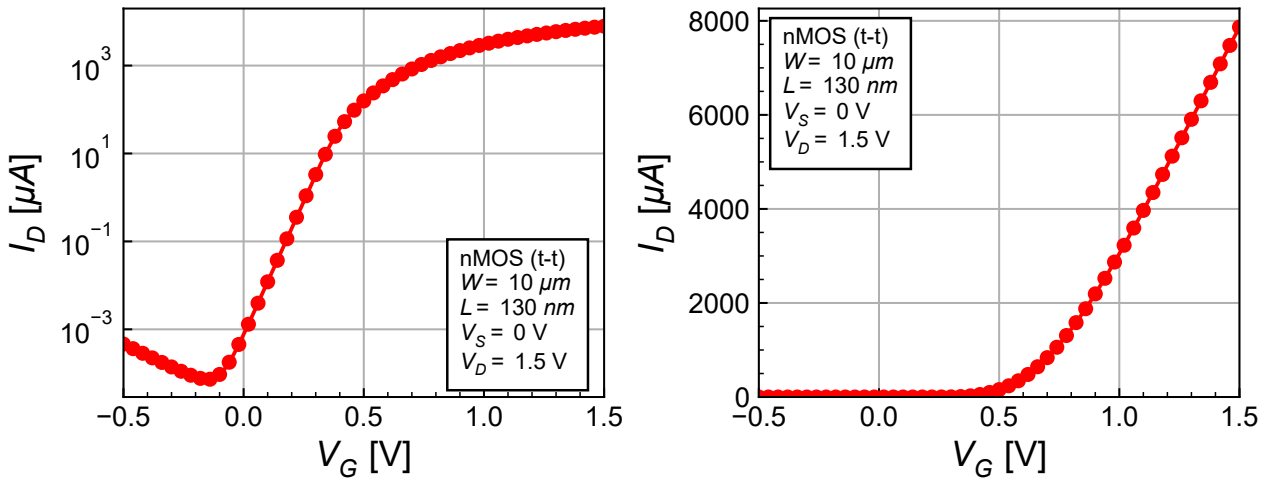

Figure 3.2: Imported I_D-V_G.

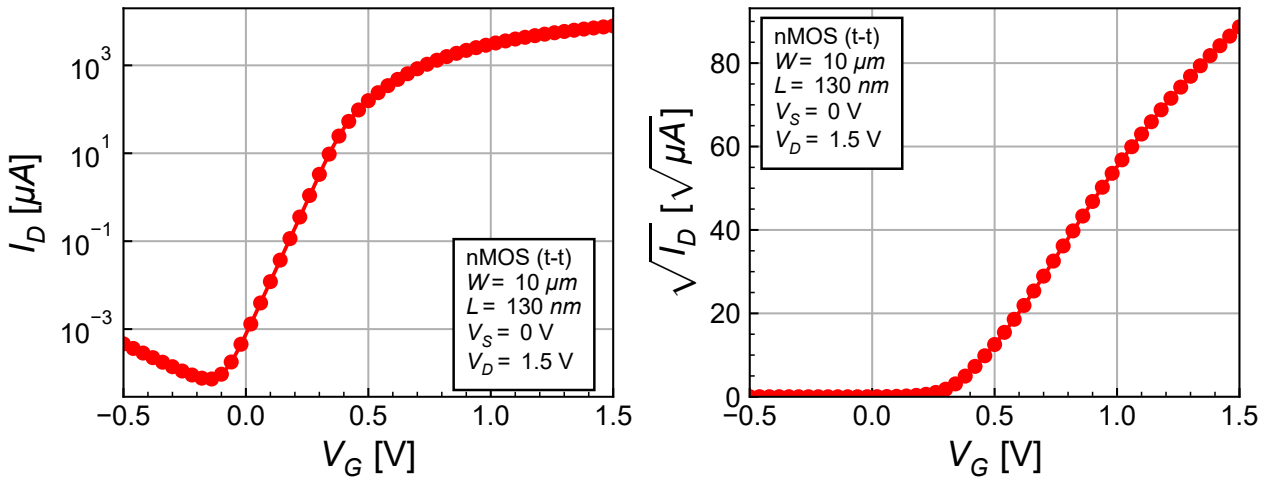

Figure 3.3: Imported I_D-V_G.

3.1.2 G_m-V_G and G_m-I_D

We now will check the derivative namely the gate transconductance obtained from the simulator and compare it to the numerical differentiation of the large-signal I_D-V_G characteristic.

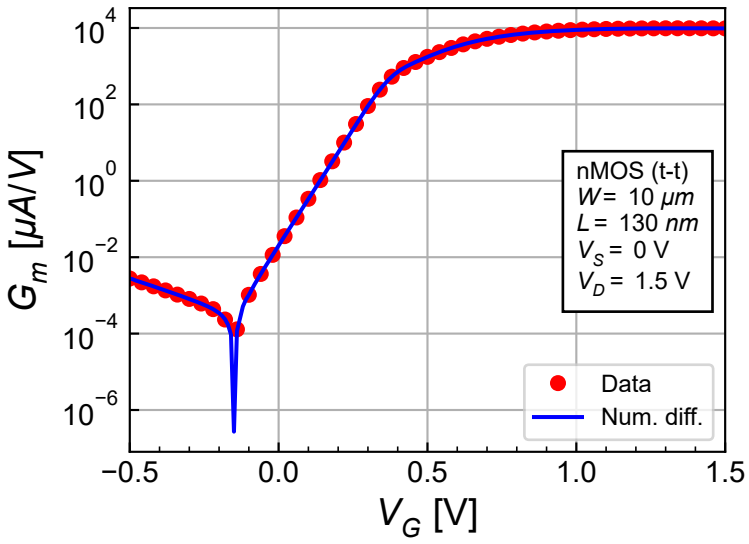

Figure 3.4: Check of the G_m-V_G consistency.

We see that the transconductance obtained by differentiating the large-signal I_D-V_G characteristic is equal to the transconductance extracted from the PSP model. We will keep the value extracted from the PSP model.

3.2 Filtering the outliers

Since the sEKV model [2] doesn't account for leakage currents such as gate induced drain leakage (GIDL) that appears at very low current, we need to filter the outlier points. This is done below with the outlier points shown in blue and the points used for the extraction shown in red.

We can now proceed with the parameter extraction, starting with the direct extraction approach with $\lambda_c = 0$.

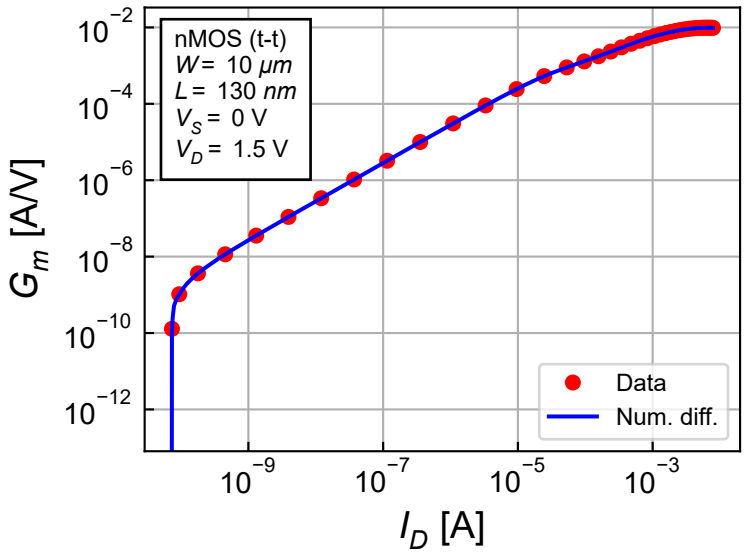

Figure 3.5: Check of the G_m-I_D consistency.

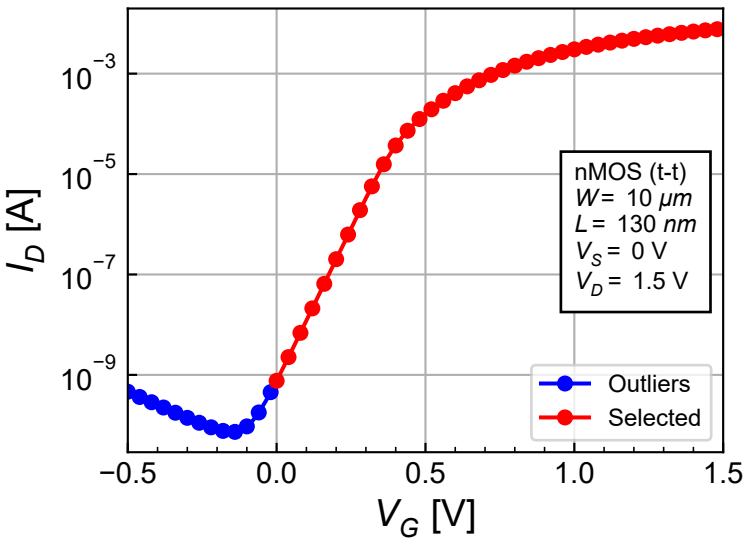

Figure 3.6: Filtering the outliers from the I_D-V_G charactersitic.

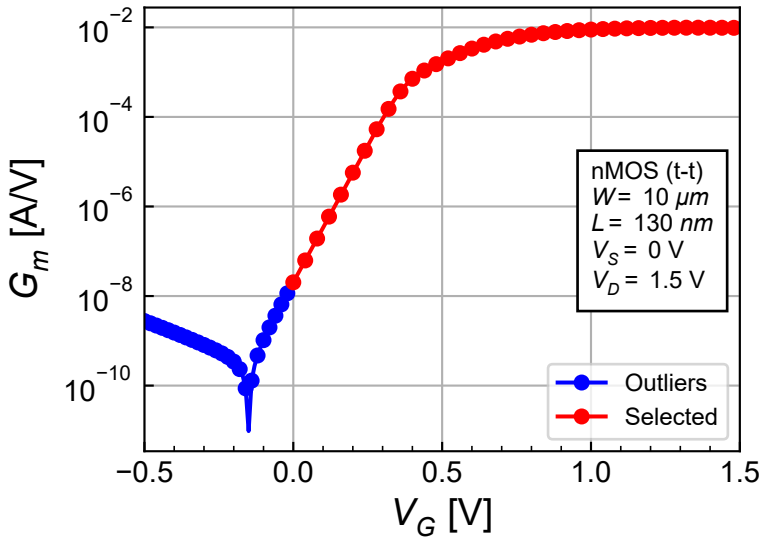

Figure 3.7: Filtering the outliers from the G_m-V_G characersitic.

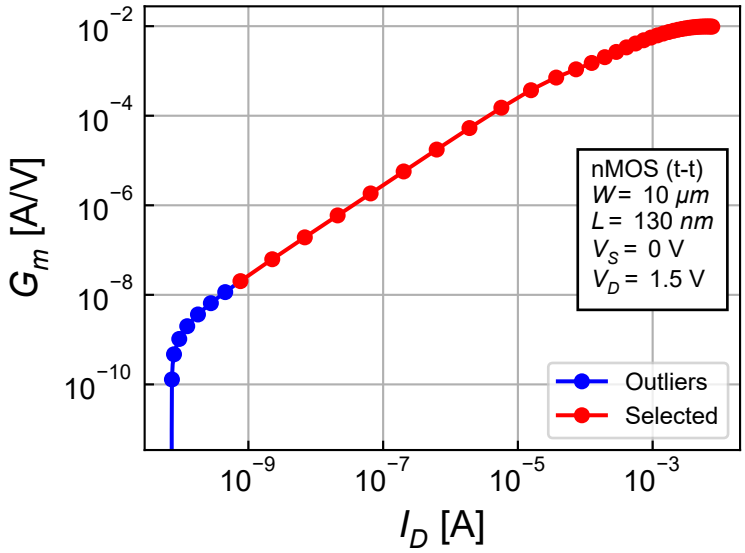

Figure 3.8: Filtering the outliers from the G_m-I_D characersitic.

3.3 Direct extraction with $\lambda_c = 0$

In the direct extraction approach, we avoid using curve fitting or optimization and manipulate the data to extract a given parameter in a certain data range. We start extracting the slope factor n and the specific current I_{spec}.

3.3.1 Slope factor n and I_{spec} extraction

Remenber that the gate transconductance in weak inversion and saturation is given by [1]

$$G_m = \frac{I_D}{n\,U_T}. \tag{3.1}$$

So if we plot $I_D/(G_m\,U_T)$ we should see a plateau in weak inversion the value of which is equal to the slope factor n as illustrated in Figure 3.9.

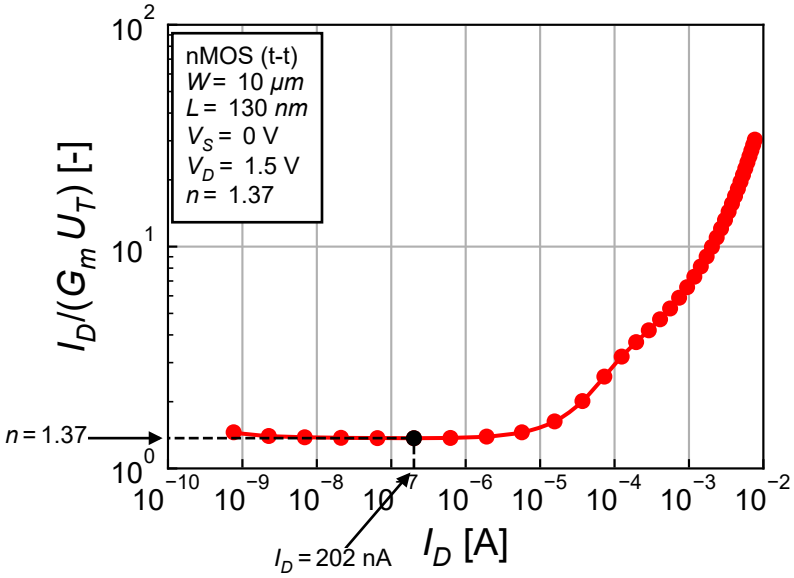

Figure 3.9: Slope factor extraction.

This is illustrated in Figure 3.9 resulting in $n = 1.37$. On the other hand the normalized G_m/I_D function for a long-channel transistor in strong inversion and saturation is given by [1]

$$\frac{G_m\,n\,U_T}{I_D} = \frac{1}{\sqrt{IC}} = \sqrt{\frac{I_{spec}}{I_D}}. \tag{3.2}$$

We can then plot $(G_m\,n\,U_T)^2/I_D$ which should find a maximum value equal to I_{spec}.

This is illustrated in Figure 3.10 resulting in $I_{spec} = 41374\ nA$ corresponding to $I_{spec\square} = 294\ nA$. We can now plot $I_D/(G_m\,U_T)$ versus I_D as shown in Figure 3.11. We clearly see the two asymptotes in weak (i.e. $I_D < I_{spec}$) and strong inversion (i.e. $I_D > I_{spec}$).

Having extracted n and I_{spec}, we can now plot the normalized G_m/I_D function versus IC which is shown in Figure 3.12.

The fit is reasonable over the entire IC span. There is some discrepancy in the moderate inversion region which is due to the mobility reduction due to the vertical field appearing for $IC > 10^2$. The latter can be accounted for by using the λ_c parameter which is normally used for modeling the effect of velocity saturation in short-channel transistors but can also be used to correct the effect of mobility reduction due to the vertical field appearing in long-channel transistors. We will not do this here since

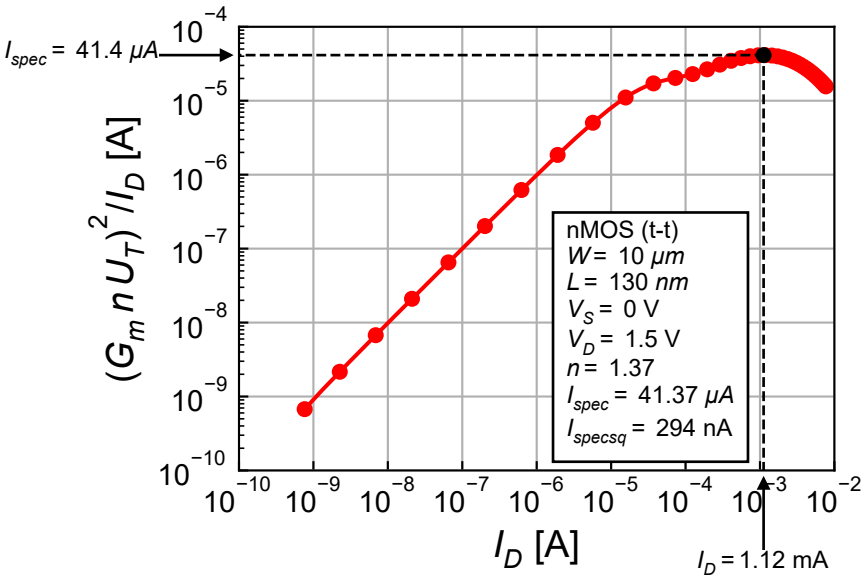

Figure 3.10: I_{spec} extraction.

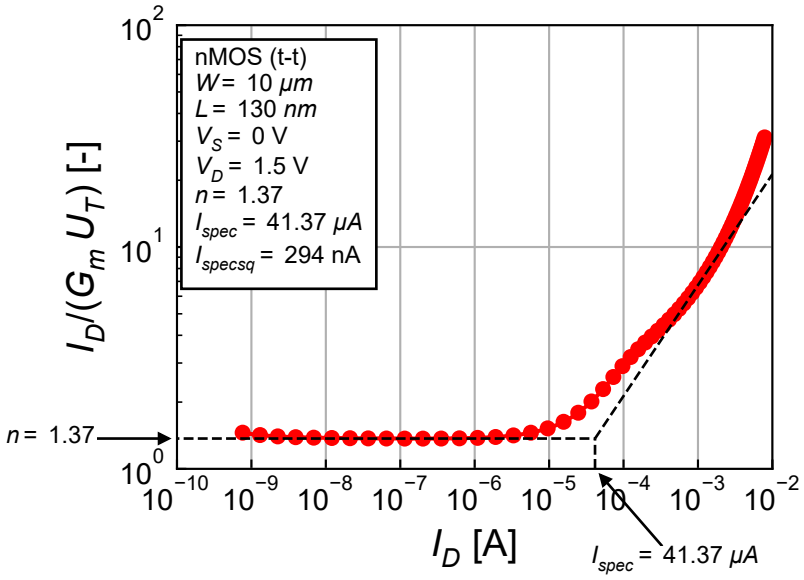

Figure 3.11: n and I_{spec} check.

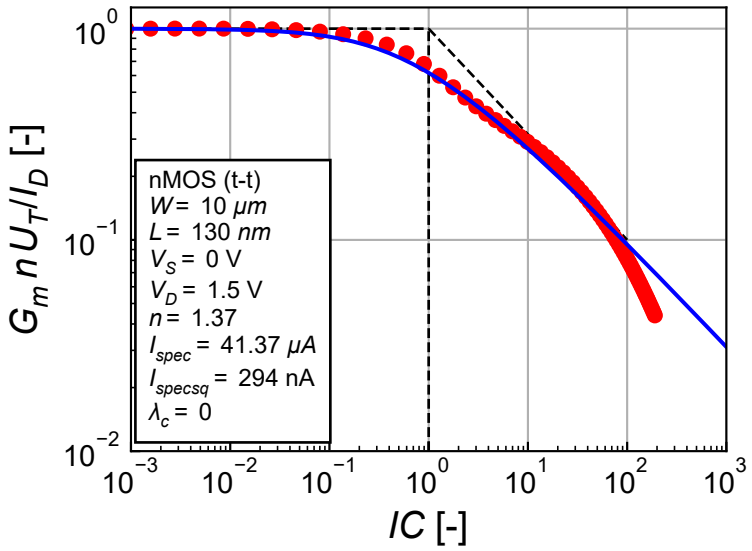

Figure 3.12: n and I_{spec} check.

we want to extract the long-channel parameters keeping $\lambda_c = 0$, but since we are mostly interested in the moderate inversion region, we can slightly increase I_{spec} to improve the fit in moderate inversion at the cost of a degradation in strong inversion. This results in the normalized G_m/I_D function versus IC shown in Figure 3.13.

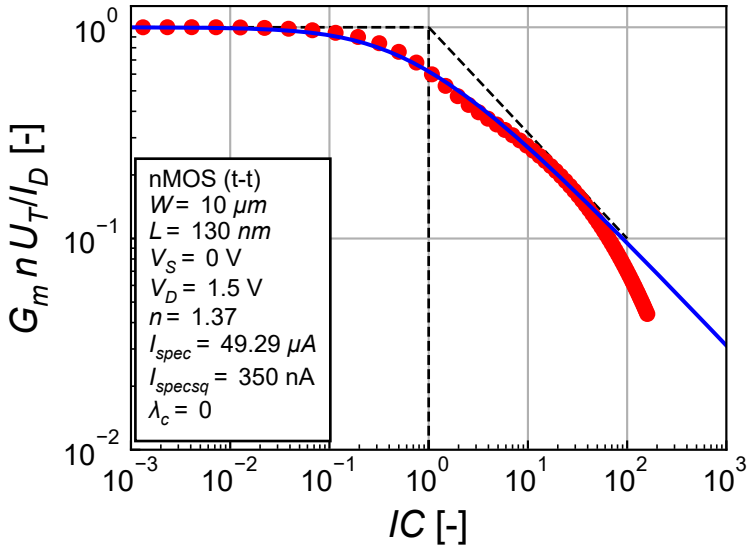

Figure 3.13: Fine tuning of the normalized G_m/I_D function versus IC in moderate inversion.

The fit is now much better in moderate inversion but less in strong inversion. This is due to mobility reduction due to the vertical field an effect that is not accounted for in the model. However, we will keep the new value of $I_{spec\square}$.

3.3.2 Threshold voltage extraction

We can extract the threshold voltage in weak inversion (assuming $V_S = 0$) from the normalized current (inversion coefficient) given by [1]

$$IC = e^{\frac{V_G - V_{T0}}{nU_T}}. \tag{3.3}$$

We can now plot

$$V_{T0} = V_G - nU_T \ln(IC) \tag{3.4}$$

to extract the threshold voltage. This results in the plot shown in Figure 3.14.

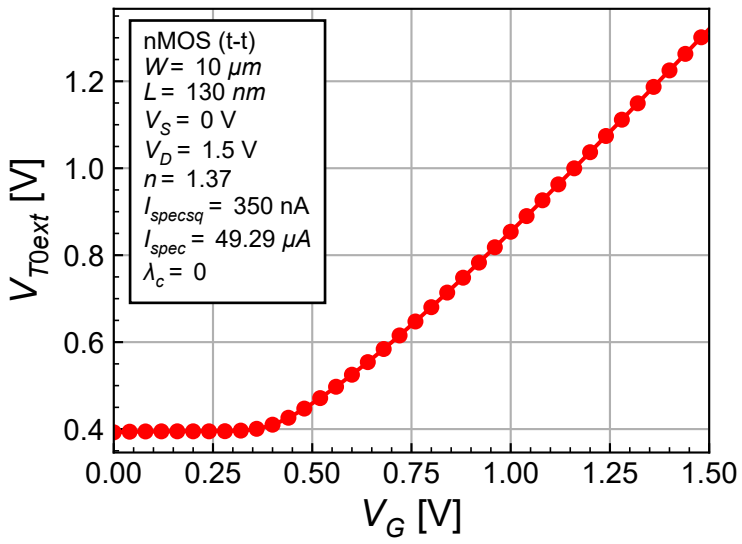

Figure 3.14: Threshold voltage extraction.

We see a plateau in weak inversion where we can average its value to get the threshold voltage in weak inversion which we can zoom into as shown in Figure 3.15.

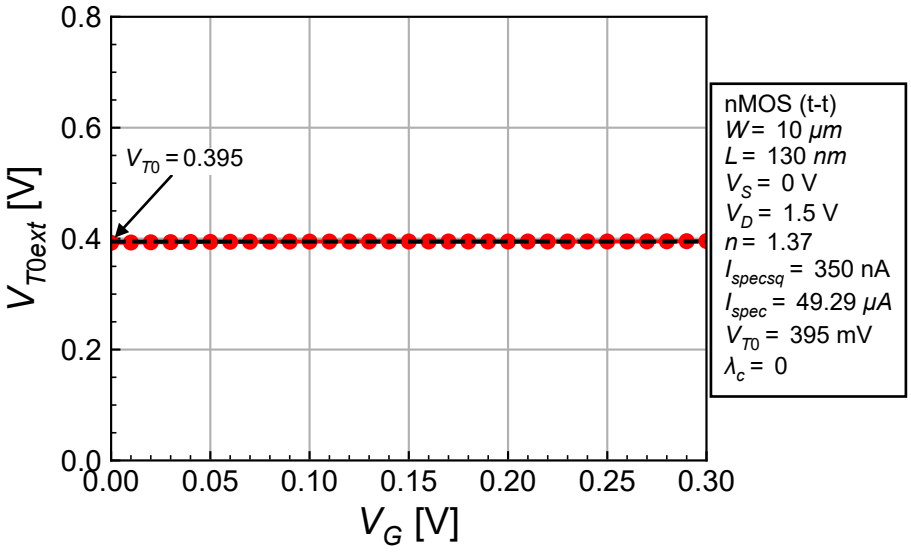

Figure 3.15: Threshold voltage extraction in weak inversion.

The average value of V_{T0} in this range is given by $V_{T0} = 395\ mV$. We can now plot the I_D-V_G for the extracted parameters which is shown in Figure 3.16.

We get a reasonable fit with some deviations in strong inversion, which is expected since we focused on the moderate inversion and kept $\lambda_c = 0$.

Note that we can also extract the threshold voltage in strong inversion by plotting $\sqrt{I_D}$ versus V_G as shown in Figure 3.17.

We can then fit the linear portion of the curve and extract the intersection point on the V_G axis as shown in Figure 3.18 which results in $V_{T0} = 366\ mV$. We can check the I_D-V_G charactersitic with this

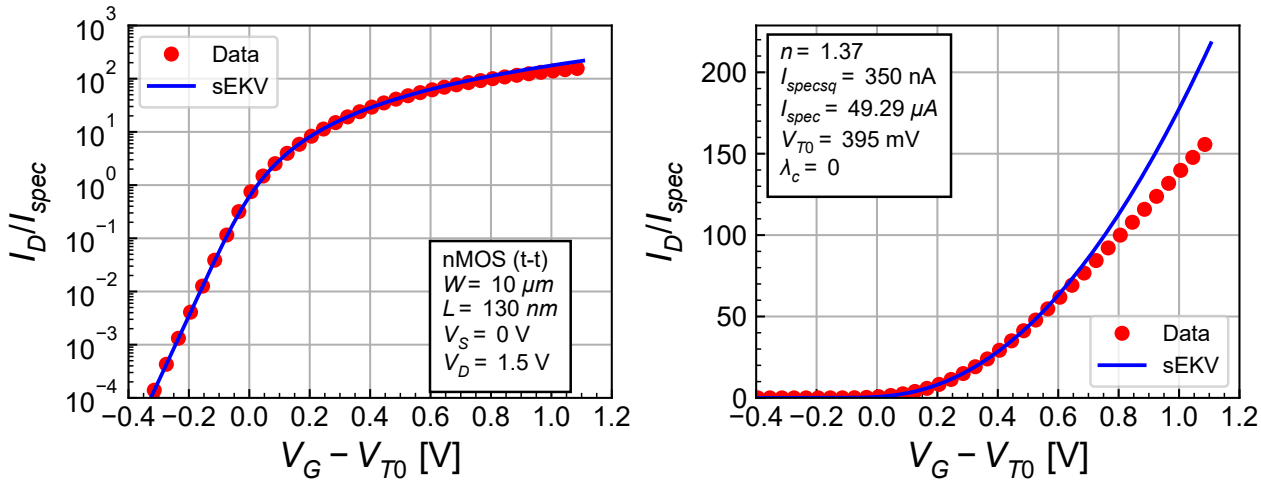

Figure 3.16: I_D-V_G for the extracted parameters.

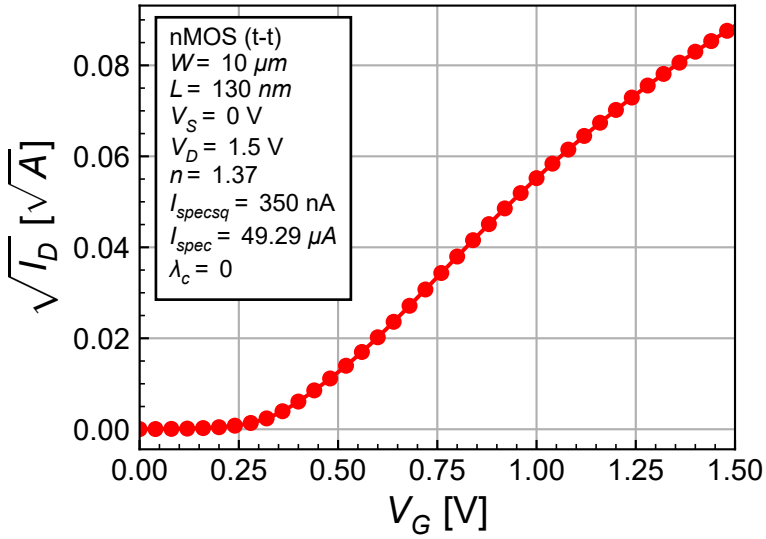

Figure 3.17: $\sqrt{I_D}$-V_G for the extracted parameters.

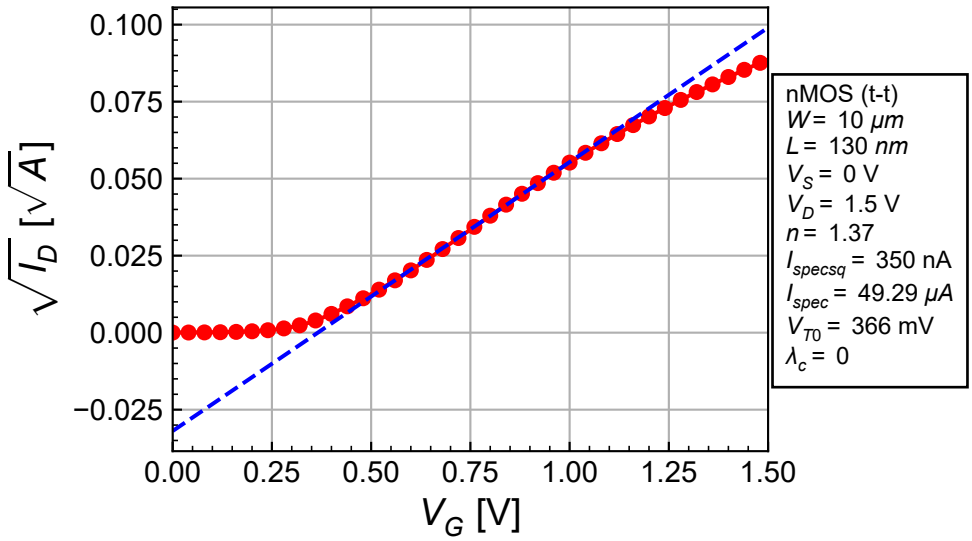

Figure 3.18: Threshold voltage extraction from $\sqrt{I_D}$-V_G in strong inversion.

extracted threshold voltage in Figure 3.19.

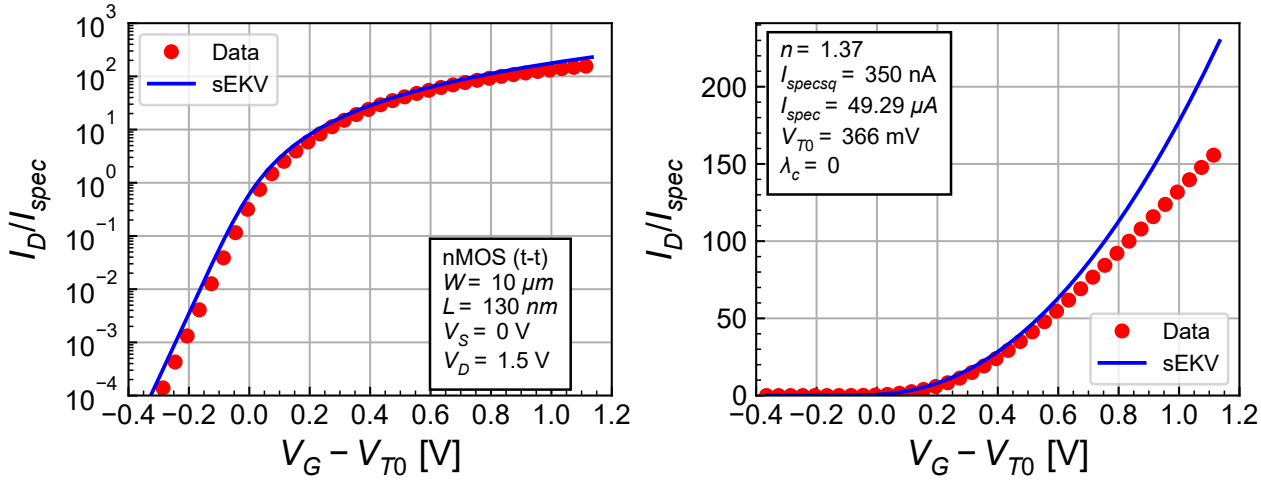

Figure 3.19: I_D-V_G for the extracted threshold voltage.

As shown in Figure 3.19, we get a less good fit in weak inversion. We therefore keep the value of the threshold voltage extracted in weak inversion, namely $V_{T0} = 395\ mV$.

3.3.3 Summary

The results of the direct extraction method is shown in Figure 3.20, which includes the large-signal $IC = I_D/I_{spec}$ versus $V_G - V_{T0}$ on the left and the small-signal parameters $G_{ms}/G_{spec} = G_m\, n\, U_T/I_{spec}$ versus IC and $G_m\, n\, U_T/I_D$ versus IC on the right. We see a good fit of the large- and small-signal parameters except in very strong inversion (i.e. $100 < IC$). The extracted parameters are summarized in Table 3.1.

Table 3.1: Direct extraction of the sEKV parameters with $\lambda_c = 0$.

Type	n	$I_{spec\square}\ [nA]$	$V_{T0}\ [mV]$	λ_c	$L_{sat}\ [nm]$	Comment
nMOS	1.37	350	395	0	0	direct with $\lambda_c = 0$

We now will use the VS λ_c to get a better fit in strong inversion.

3.4 Direct extraction with $\lambda_c > 0$

3.4.1 Slope factor n extraction

Proceeding in the same way as above, we can extract the slope factor n from the characteristic shown in Figure 3.21.

We get the same value as before namely $n = 1.37$.

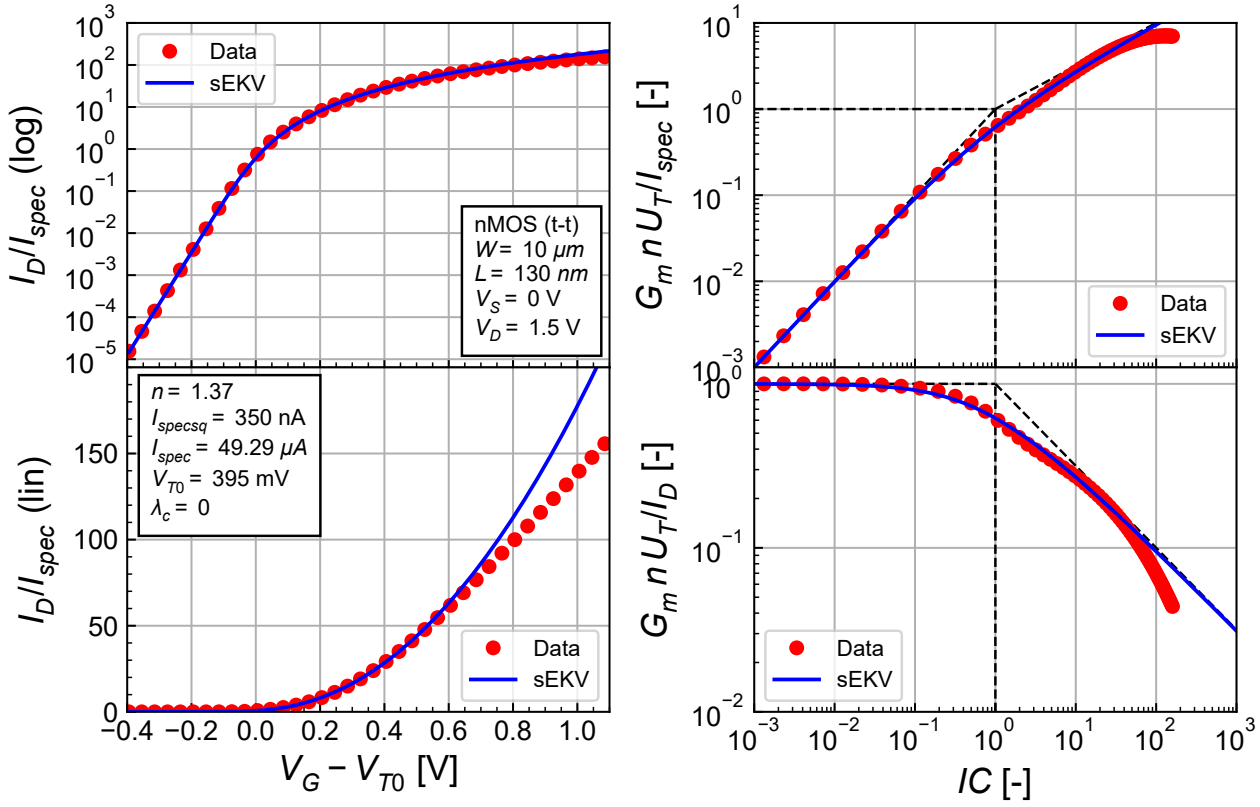

Figure 3.20: Summary of direct extraction with $\lambda_c = 0$.

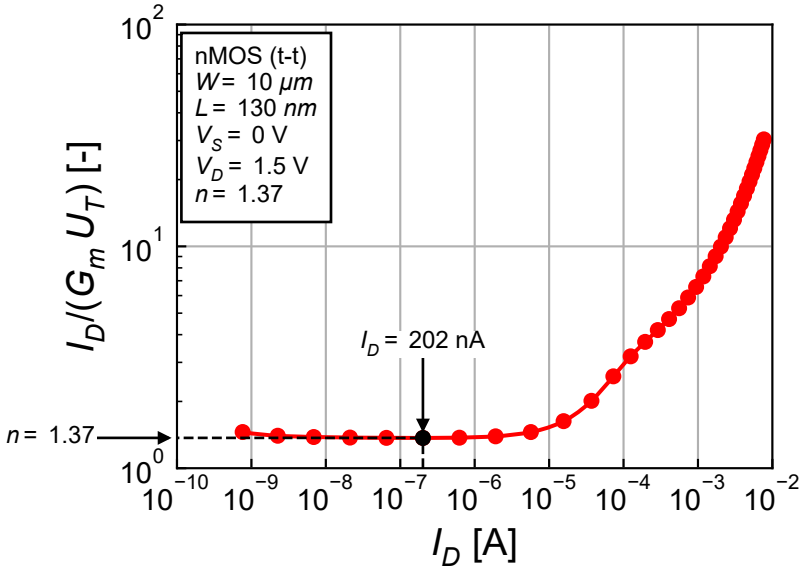

Figure 3.21: Slope factor extraction.

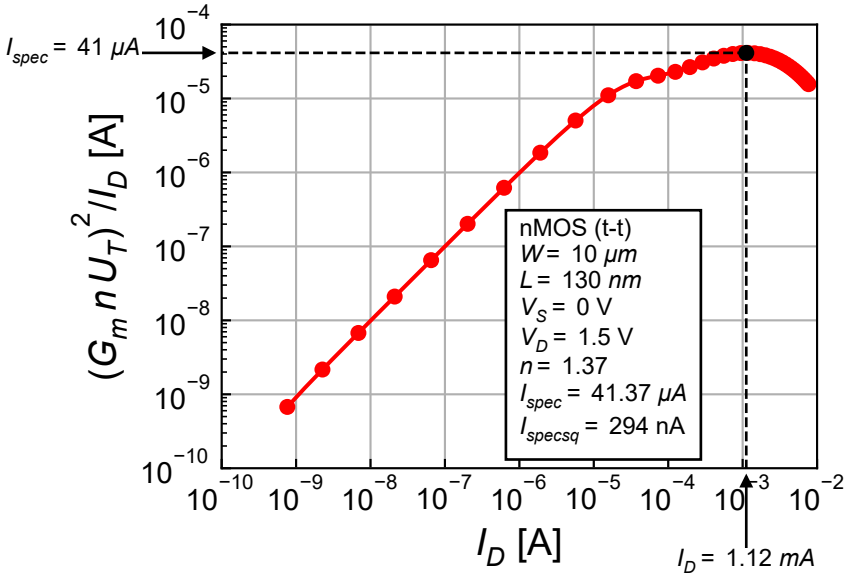

Figure 3.22: I_{spec} extraction.

3.4.2 Specific current I_{spec} extraction

The specific current is extracted as above from the characteristic shown in Figure 3.22.

We of course get the same value as before, namely $I_{spec} = 41.37\ \mu A$ corresponding to $I_{spec\square} = 294\ nA$. We can the plot $I_D/(G_m U_T)$ as shown in Figure 3.23. We see that the asymptote are correct except in strong inversion where the curve is steeper. This can then be handled by the additional VS parameter λ_c.

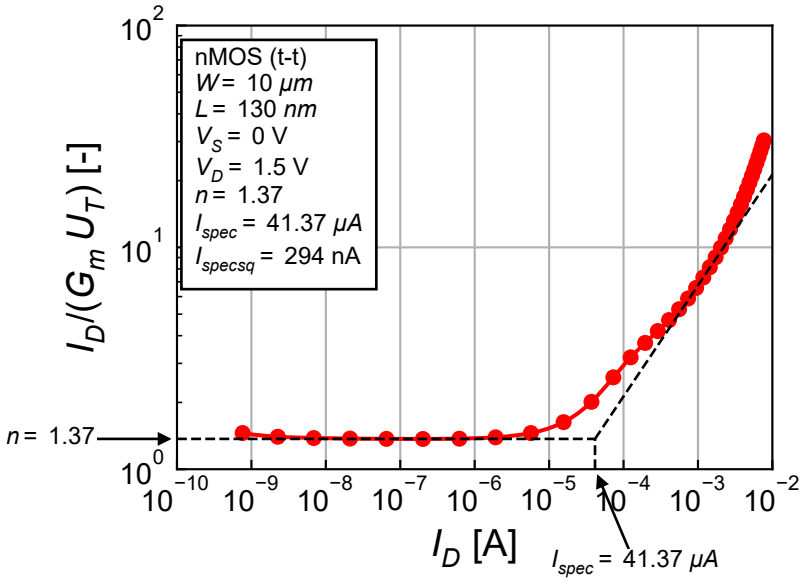

Figure 3.23: n and I_{spec} check.

3.4.3 Velocity saturation parameter λ_c extraction

We can extract λ_c by looking at the asymptote in very strong inversion. For a short-channel transistor in strong inversion and saturation, the normalized G_m/I_D is given by [1]

$$\frac{G_m\, n\, U_T}{I_D} = \frac{1}{\lambda_c\, IC} = \frac{I_{spec}}{\lambda_c\, I_D}. \tag{3.5}$$

So if we plot $I_{spec}/(G_m\, n\, U_T)$ it will have a minimum at λ_c as illustrated in Figure 3.24.

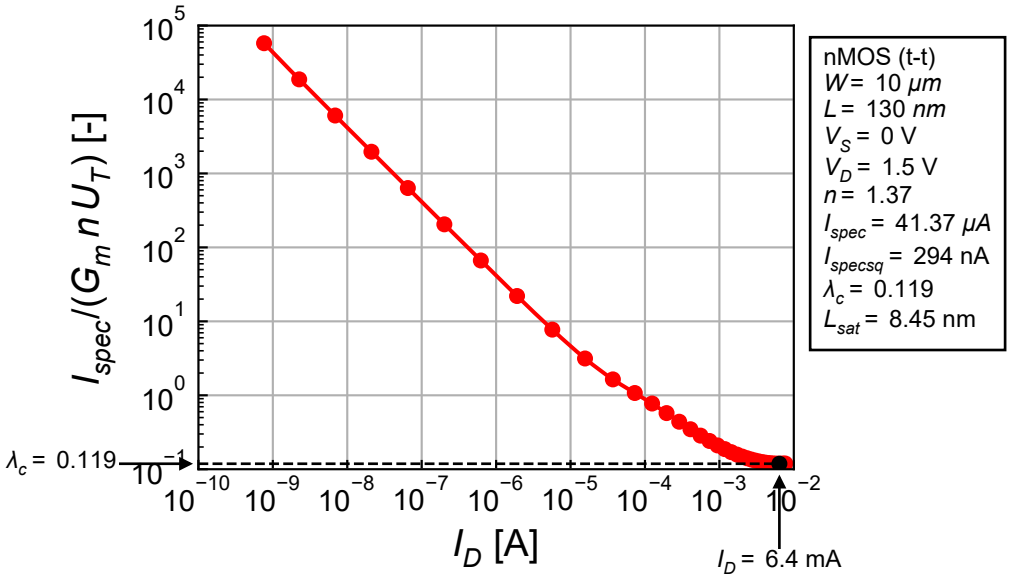

Figure 3.24: Extraction of λ_c.

This results in $\lambda_c = 0.119$ corresponding to $L_{sat} = 8.45\ nm$. We can now add the strong inversion asymptote on the $I_D/(G_m\, n\, U_T)$ versus I_D characteristic as shown in Figure 3.25.

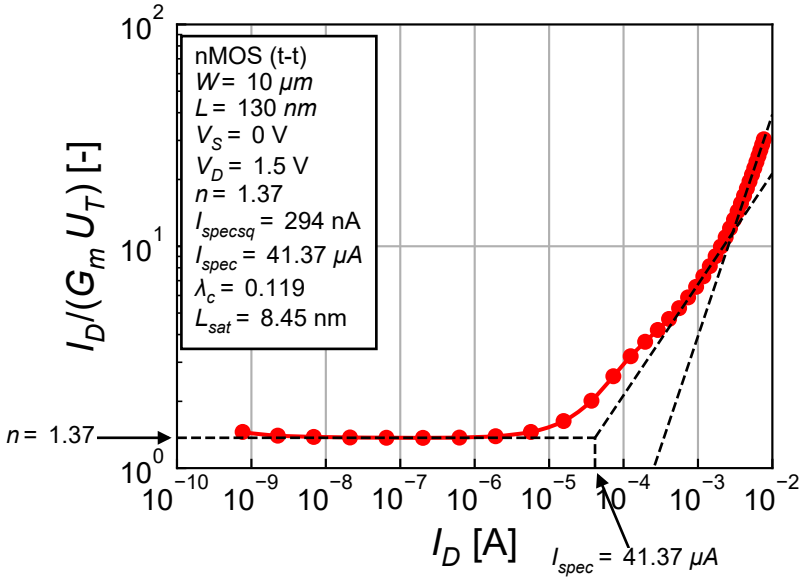

Figure 3.25: n, I_{spec} and λ_x check.

We can also check the normalized G_m/I_D characteristic which is plotted in Figure 3.26.

The fit is OK at the asymptotes but not good in the moderate and strong inversion regions. Notice the bump in the lower part of strong inversion. This is most probably an artifact of the PSP model.

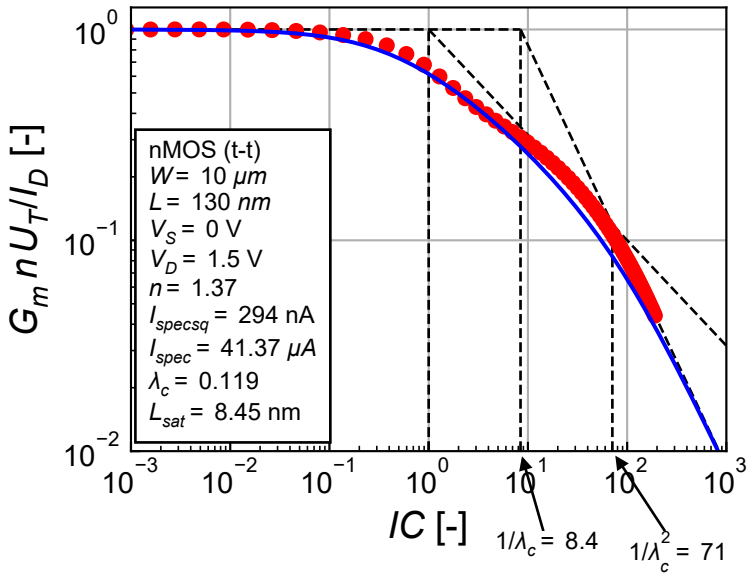

Figure 3.26: Check of the normalized G_m/I_D for n, I_{spec} and λ_c.

We can try to increase I_{spec} and λ_c in order to have a better fit in moderate and strong inversion as illustrated in Figure 3.27.

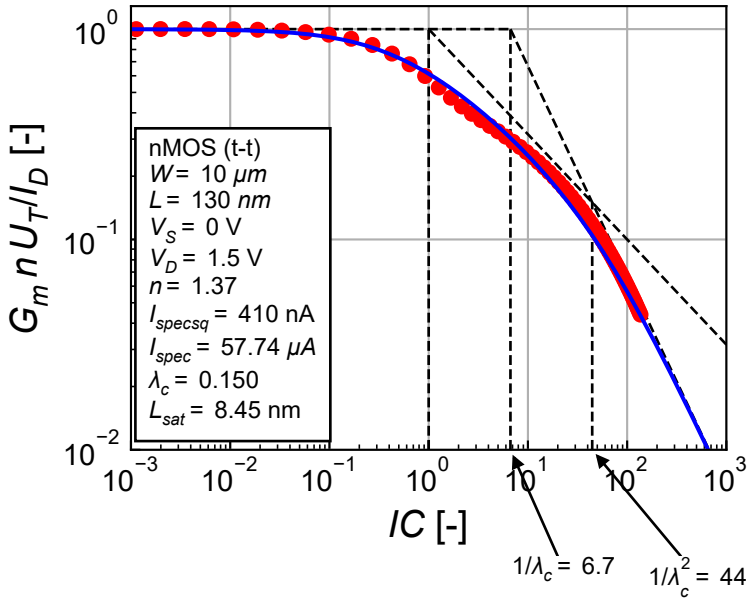

Figure 3.27: Tuning of I_{spec} and λ_c on the normalized G_m/I_D.

The fit is now better, offering a good trade-off between moderate and strong inversion.

3.4.4 Threshold voltage extraction

We now extract the threshold voltage in the same way as above, first plotting V_{T0ext} versus V_G as shown in fig-vt0ext_vg.

Averaging the threshold voltage in the range it is about constant results in $V_{T0} = 389\ mV$ which is slightly lower than the value extracted with $\lambda_c = 0$. We can now check the I_D-V_G curves which are shown in Figure 3.30.

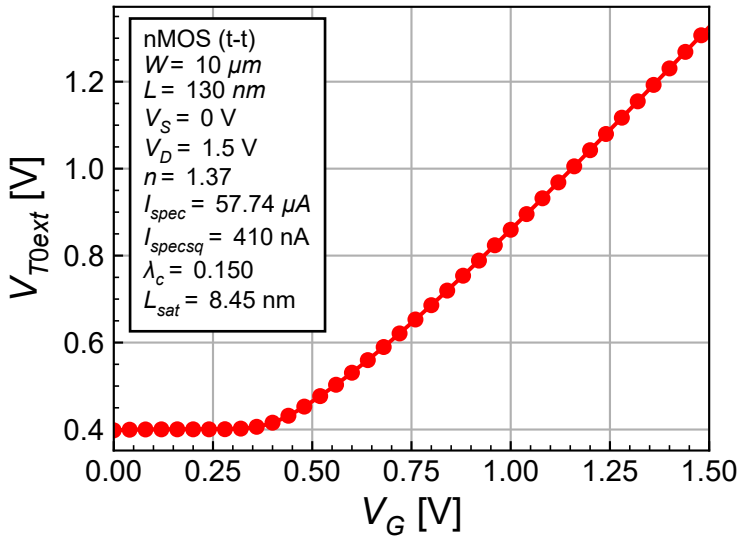

Figure 3.28: Threshold voltage extraction.

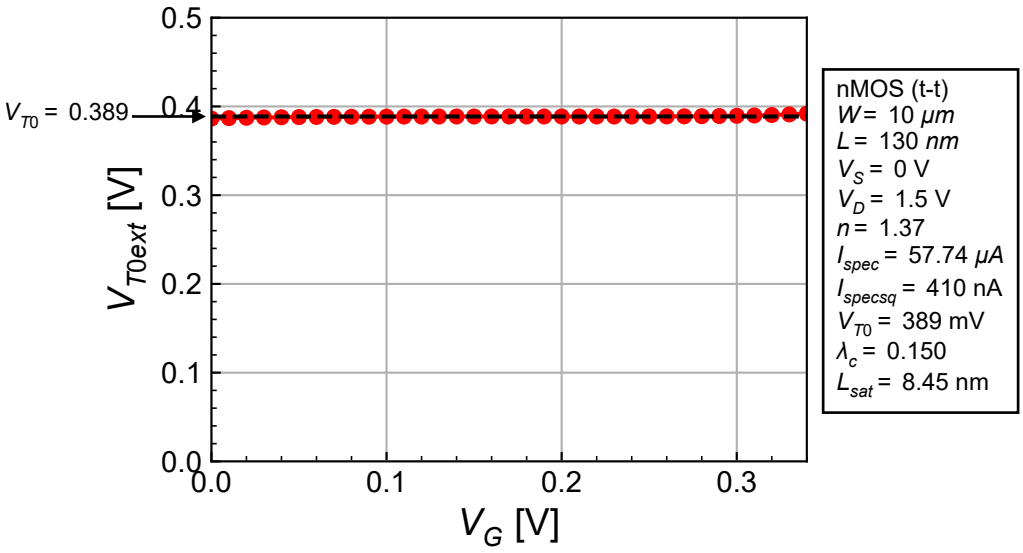

Figure 3.29: Threshold voltage extraction in weak inversion.

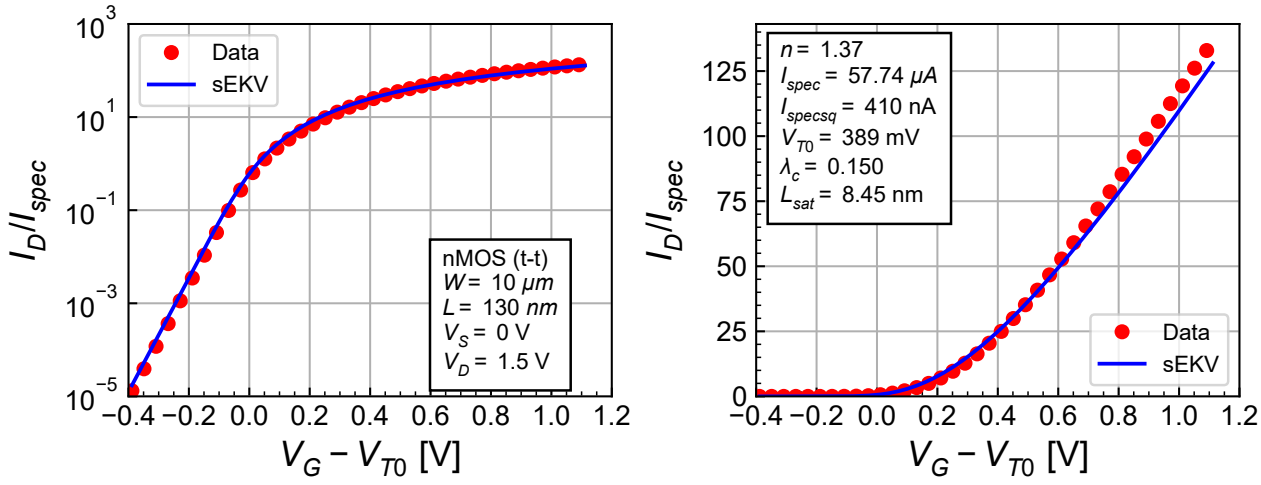

Figure 3.30: I_D-V_G for the extracted parameters.

We see that the threshold voltage is too low. We can fine tune it manually as illustrated in Figure 3.31.

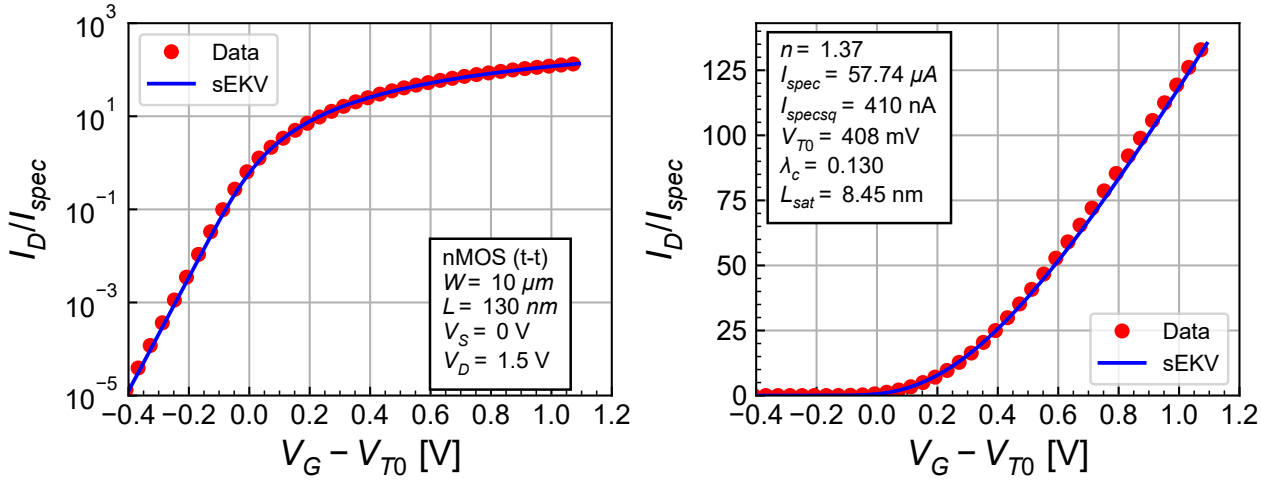

Figure 3.31: I_D-V_G for the extracted parameters.

With $V_{T0} = 408\ mV$, we now have a very good fit of the I_D-V_G characteristic in the entire range of $V_G - V_{T0}$, from weak to strong inversion.

3.4.5 Summary

We results of the direct extraction with $\lambda_c > 0$ are summarized in Figure 3.32 for the sEKV parameters presented in Table 3.2.

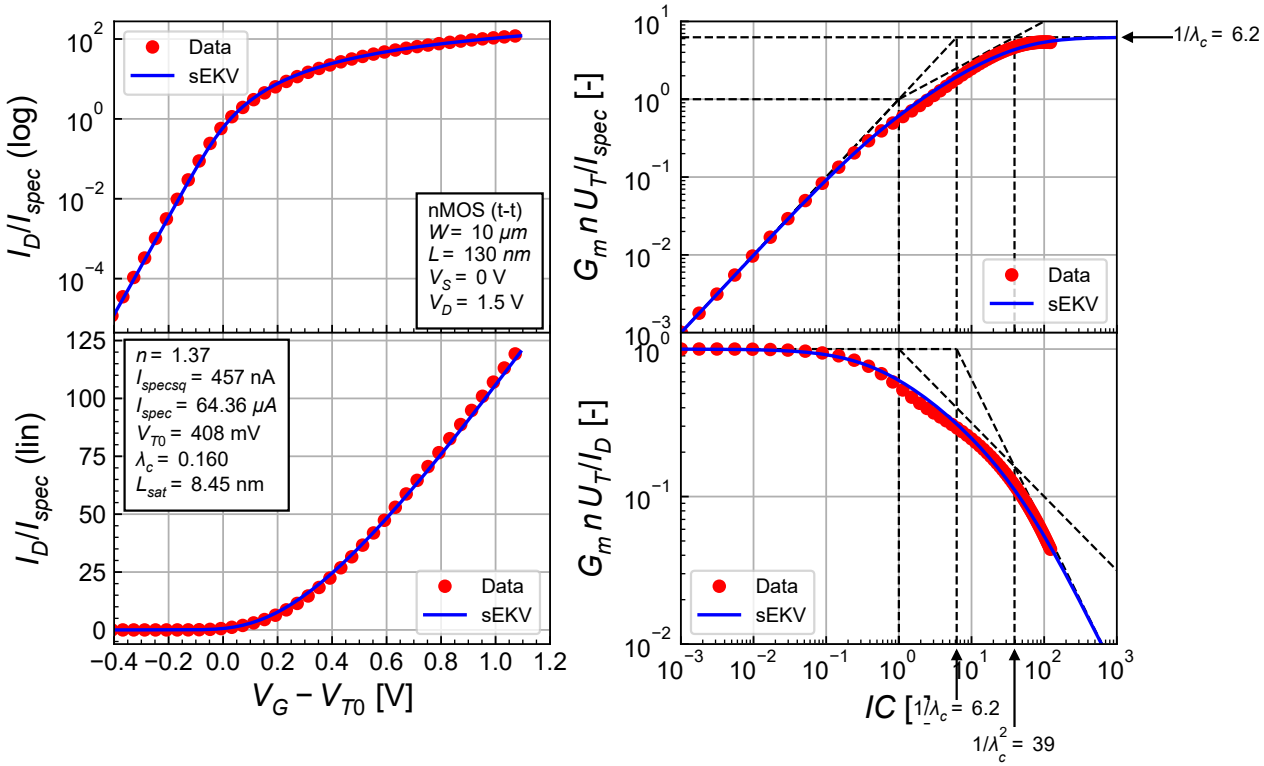

Figure 3.32: Summary of the direct extraction with $\lambda_c > 0$.

We finally get a reasonable fit of all characteristics.

Table 3.2: Extraction of the sEKV parameters using direct extraction with $\lambda_c > 0$.

Type	n	$I_{spec\square}$ $[nA]$	V_{T0} $[mV]$	λ_c	L_{sat} $[nm]$	Comment
nMOS	1.37	350	395	0.00	0.00	direct with $\lambda_c = 0$
nMOS	1.37	457	408	0.16	8.45	direct with $\lambda_c > 0$

3.5 Extraction using curve fitting

3.5.1 Specific current I_{spec} and λ_c extraction

We can extract the slope factor n, the specific current I_{spec} and the velocity saturation parameter λ_c on the normalized G_m/I_D versus IC characteristic using curve-fitting. The result is shown in Figure 3.33.

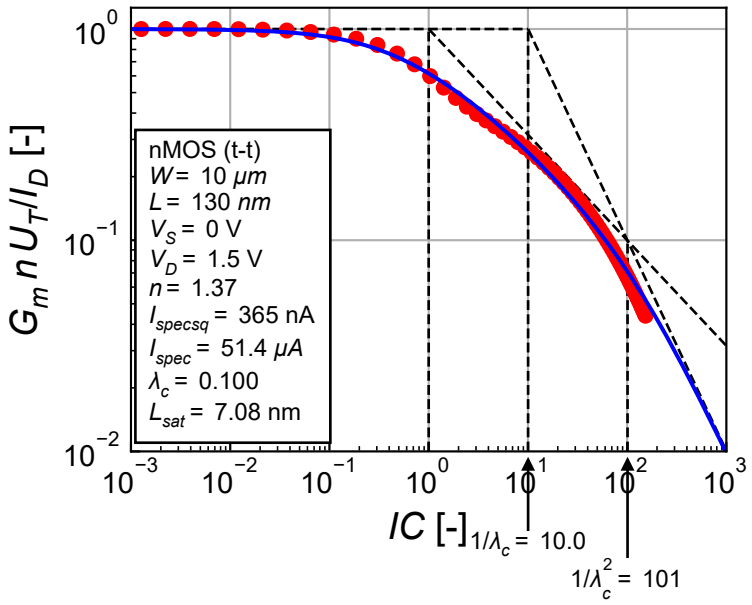

Figure 3.33: Extraction of n, I_{spec} and λ_c by curve fitting.

We get a good fit across all regions with similar values than the one obtained in the direct extraction methodology.

3.5.2 Threshold voltage extraction

We can also extract the threshold voltage from the I_D-V_G charactersitic as illustrated in Figure 3.34.

This results in $V_{T0} = 395\ mV$ which is close to what was obtained with the direct extraction. Figure 3.34 shows that curve fitting can result in a very good fit in all regions of operation!

3.5.3 Summary

The result of the curve fitting extraction methodology is summarized in Figure 3.35 with the paramters given in Table 3.3. We see that we obtained an overall good fit in all regions of operation.

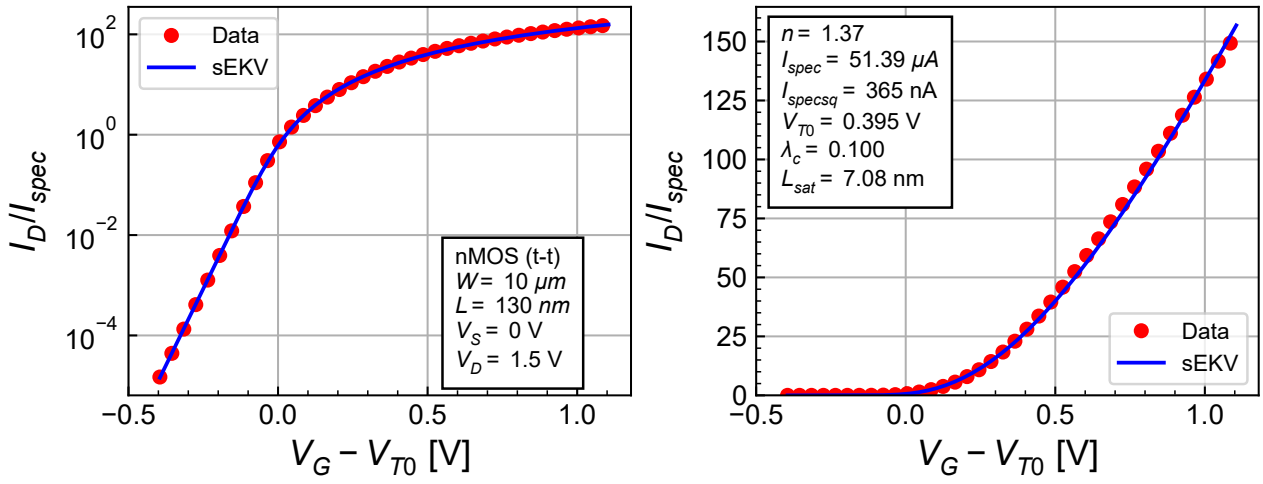

Figure 3.34: Threshold voltage extraction.

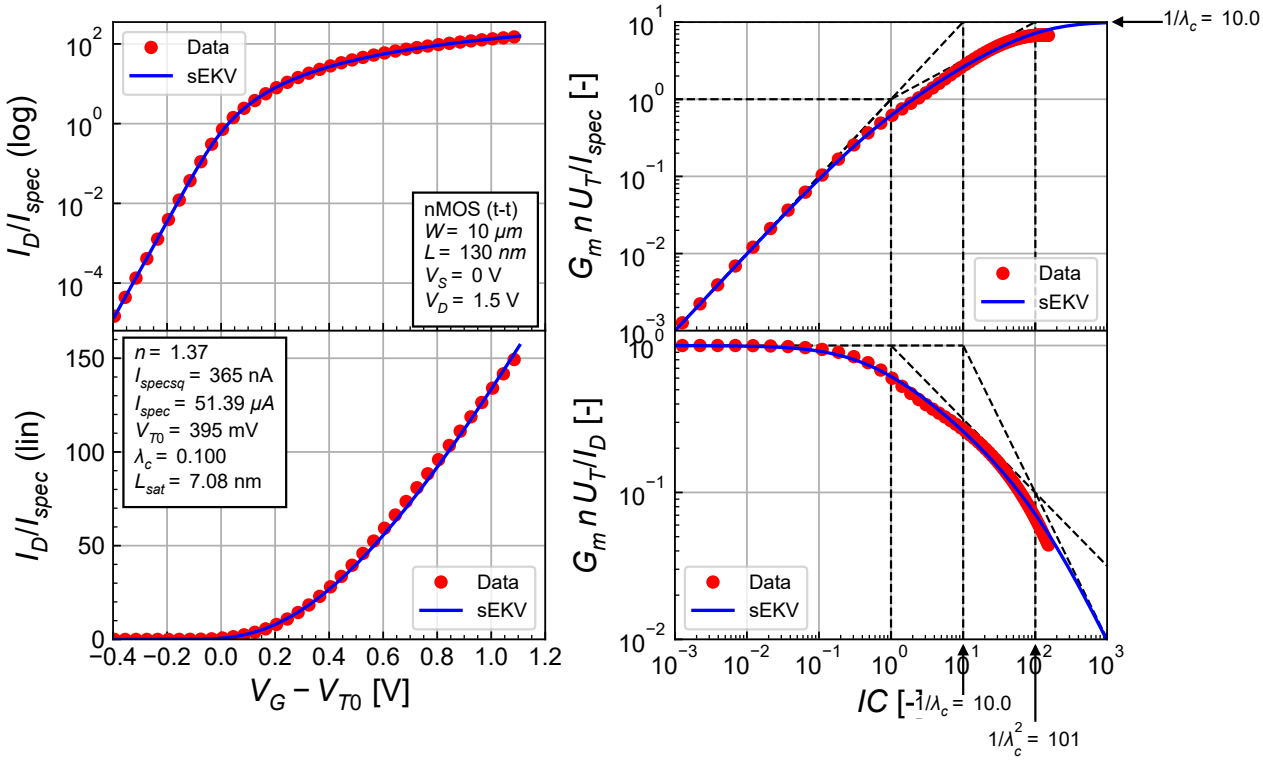

Figure 3.35: Summary of extraction by curve fitting for the long-channel.

Table 3.3: Extraction of the sEKV parameters using curve fitting with $\lambda_c > 0$.

Type	n	$I_{spec\square}$ $[nA]$	V_{T0} $[mV]$	λ_c	L_{sat} $[nm]$	Comment
nMOS	1.37	350	395	0.000	0.000	direct with $\lambda_c = 0$
nMOS	1.37	457	408	0.160	8.447	direct with $\lambda_c > 0$
nMOS	1.37	365	395	0.100	7.083	curve fitting with $\lambda_c > 0$

4 Output characteristic

4.1 Generating and importing the data

The data used for the sEKV parameters extraction is generated by simulation using the PSP CM [4] from the PDK of the IHP 130nm process [3] for the typical-typical (t-t) case. We present the I_D-V_G and G_m-V_G data below.

4.1.1 I_D and G_{ds} versus V_D

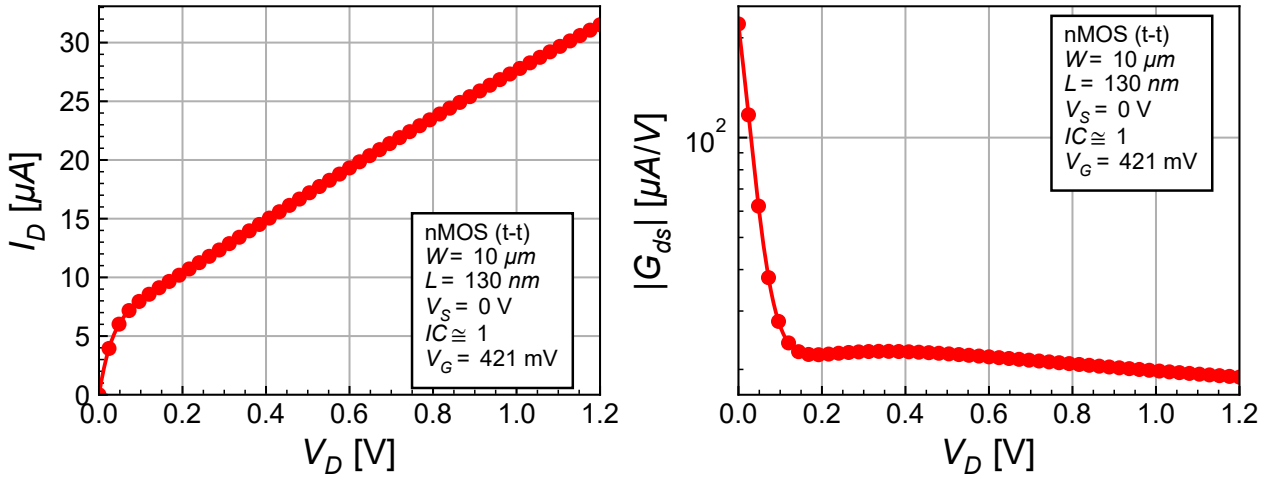

Figure 4.1: Imported I_D-V_D and G_{ds}-V_D.

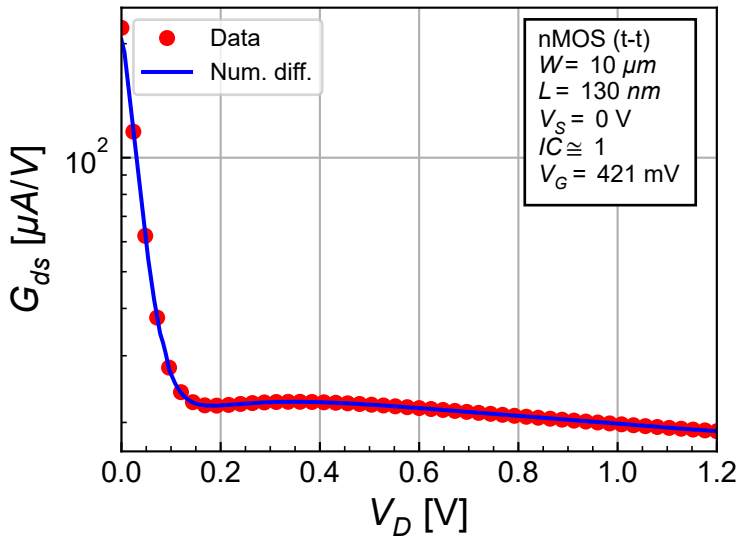

Figure 4.2: Check imported G_{ds} against computed G_{ds}.

The output conductance calculated by differentiating the large-signal I_D-V_D matches the value extracted from the PSP model. We will keep the value from PSP.

4.2 Filtering the outliers

In order to extract the CLM parameter in saturation, we will now filter out the points that correspond to the linear region. We can do this easily by looking at the G_{ds} versus V_D characteristic as shown in Figure 4.3.

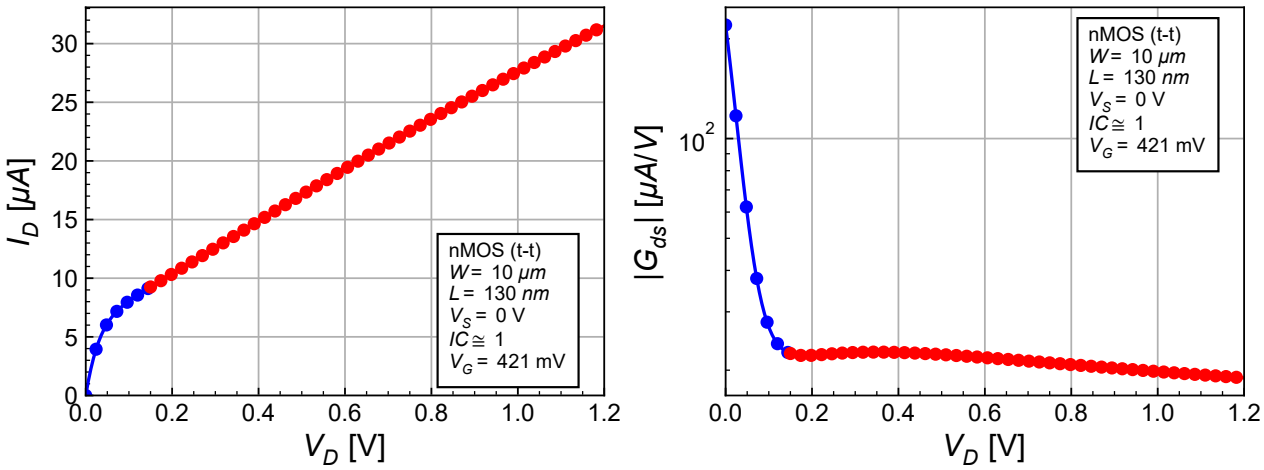

Figure 4.3: Filtering the outliers from I_D-V_G and G_{ds}-V_D.

4.3 Extracting the CLM parameter

The simple channel length modulation (CLM) of the output conductance in saturation is approximated by

$$G_{ds} = \frac{I_{D,sat}}{V_E} \tag{4.1}$$

where $I_{D,sat}$ is the drain current in saturation and

$$V_E = \lambda \cdot L_{eff} \tag{4.2}$$

is the Early voltage or CLM voltage which is proportionnal to the effectve length. This corresponds to a linear approximation of the drain current in saturation given by

$$I_{D,sat} \cong G_{ds} \cdot (V_D - V_E) \tag{4.3}$$

The value I_{D0} corresponds to the intercept

$$I_{D0} = -G_{ds} \cdot V_E \tag{4.4}$$

which is positive since V_E is negative.

The linear regression approximation of the drain current in saturation is shown in Figure 4.4 by the dashed black line. We get a rather high output conductance $G_{ds} = 21.324\ \mu A/V$ and hence low value of the λ parameter with $\lambda = 2.288\ V/\mu m$ for such a long transistor! This translates into a poor intrinsic voltage gain G_m/G_{ds}. The output conductance parameters are summarized in Table 4.1.

As shown in the right plot of Figure 4.4, the output conductance is approximated by a constant value represented by the dashed black line. It is a poor approximation of the output conductance

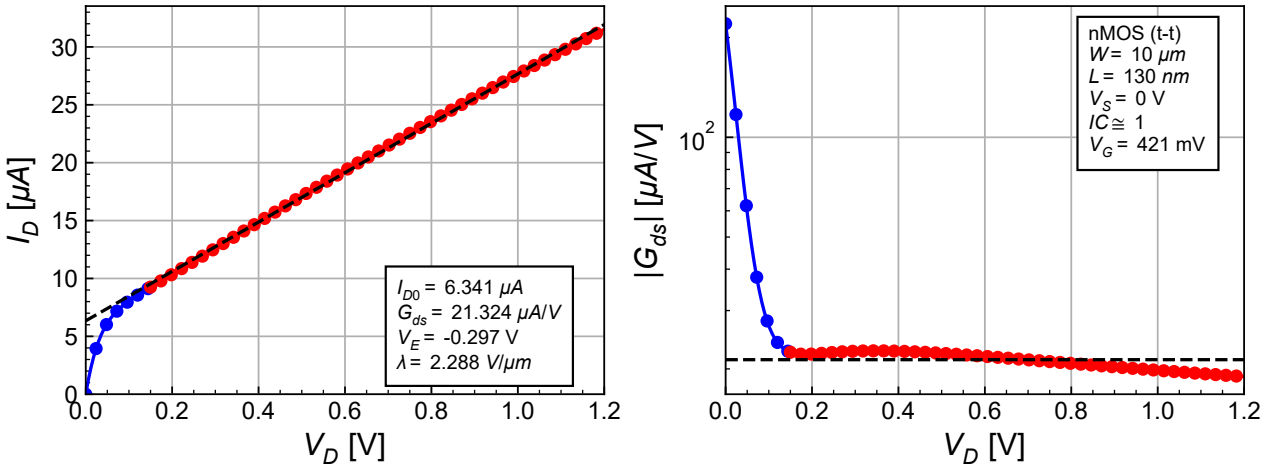

Figure 4.4: Extraction of the CLM parameter λ.

but good enough for starting a design. Note that, in analog circuit design, having a good fit of the output conductance is less important than having a good fit of the transconductance because often we just need the intrinsic voltage gain to be large enough for the circuit to perform correctly, while we want to have a good estimation of the parameters depending on the transconductance, such as the gain-bandwidth product or the thermal noise.

Table 4.1: CLM parameters extracted in moderate inversion.

Type	L_{eff} [μm]	IC	G_{ds} [$\mu A/V$]	I_{D0} [μA]	V_E [V]	λ [$V/\mu m$]	Comment
nMOS	0.071	1	21.324	6.341	-0.297	2.288	extracted in MI

5 Noise

In this section we will check the white noise power spectral density (PSD) and extract the flicker noise parameters to be used with sEKV. We reuse the flicker noise model from EKV 2.6, where the input (gate) referred PSD is given by [7]

$$S_{nin,fl}(f) = \frac{KF}{W_{eff}\, L_{eff}\, C_{ox}\; f^{AF}} \tag{5.1}$$

In this model the flicker noise is assumed to scale as $1/C_{ox}$, which is correct if the noise follows the Hooge model (i.e. originates from mobility fluctuations). In the case of the Mc Worther model (i.e. flicker noise originating from traps in the Si-SiO_2 interface and in the oxyde), the PSD scales as C_{ox}^2. Despite the flicker noise is usually dominated by the trapping mechanism, we will keep the above model with a $1/C_{ox}$ scaling.

In EKV, we like to rewrite the flicker noise PSD like the thermal noise in terms of an input-referred noise resistance

$$S_{nin,fl}(f) = 4kT\, R_{nin,fl}(f) \tag{5.2}$$

which obviously depends on frequency according to

$$R_{nin,fl}(f) = \frac{\rho}{W_{eff}\, L_{eff}\, f^{AF}} \tag{5.3}$$

with parameter ρ defined as

$$\rho = \frac{KF}{4kT\, C_{ox}}. \tag{5.4}$$

Note that the flicker noise parameter have some weird units. Indeed, KF is in $A \cdot V \cdot s^{2-AF}$ and ρ is in $V \cdot m^2/(A \cdot s^{AF})$. If $AF = 1$, like it is often the case, then KF is in $A \cdot V \cdot s$ and ρ is in $V \cdot m^2/(A \cdot s)$.

To extract the noise parameters, we use a common-source stage loaded by a noiseless resistor. We first will set the bias condition in terms of IC and calculate the input-referred white noise to compare it to the result obtained from the PSP simulations.

5.1 Setting the bias conditions

Having extracted n, $I_{spec\square}$ and V_{T0}, we can impose the inversion coefficient and calculate the corresponding gate voltage V_G. We nee to make sure the transistor remains in saturation.

We need to check that the transistor is biased in saturation. Setting the inversion coefficient to $IC = 1$ we get a drain current $I_D = 51391\ nA$ corresponding to a gate voltage $V_G = 422\ mV$. The gate transconductance is estimated at $G_m = 896.493\ \mu A/V$. Setting the voltage gain to $A_v = G_m \cdot R_L = 10$ we get $R_L = 11.155\ k\Omega$. For $V_{DD} = 1.2\ V$ we have $V_{DS} = 627\ mV$. With a saturation voltage $V_{DSsat} = 116\ mV$, the transistor is biased in the saturation region.

We can now proceed with the noise simulation and extract the PSP parameters and the PSD.

5.2 Extract operating point information

We can now check the operating point and extract the PSP noise parameters. The PSP operating point information are given in Table 5.1 and the PSP noise parameters are given in Table 5.2.

Table 5.1: PSP operating point.

Transistor	W_{eff} $[\mu m]$	L_{eff} $[\mu m]$	I_{DS} $[\mu A]$	G_m $[\mu A/V]$	G_{ds} $[\mu A/V]$	Comment
Mn	10.020	0	35.927	647.436	29.643	extracted from PSP

Table 5.2: MOS PSP noise parameters.

Transistor	$\sqrt{S_{ninth}}$ $[nV/\sqrt{Hz}]$	$\sqrt{S_{ninfl}(1kHz)}$ $[nV/\sqrt{Hz}]$	f_k $[MHz]$	Comment
Mn	4.5	230.5	2675.615	extracted from PSP

We see that the simulated bias current $I_D = 35.93\ \mu A$ is lower than the desired current $I_D = 51.39\ \mu A$ resulting in a smaller simulated transconductance $G_m = 647.44\ \mu A/V$ compared to the predicted one $G_m = 896.49\ \mu A/V$. This will lead to a higher simulated white noise compared to the predicted one.

We can re-estimate the EKV transconductance from the simulated current. The inversion coefficient corresponding to the simulated current is $IC = 0.699$ instead of $IC = 1.000$. This gives $G_m = 687.88\ \mu A/V$ which is much closer to the PSP simulated value $G_m = 647.44\ \mu A/V$.

5.3 Simulating noise PSD

We can now simulate the PSD and check against the EKV model. The square roots of the PSD are plotted versus frequency in Figure 5.1.

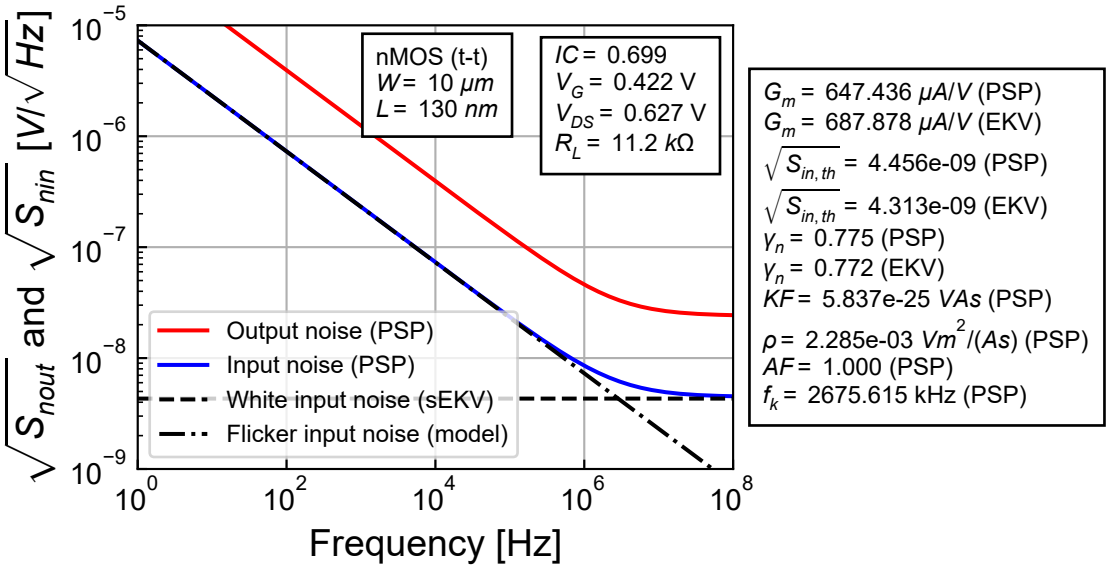

Figure 5.1: Output and input-referred PSD.

After the update of the inversion coefficient and transconductance, we see that the PSP white noise is very close to the sEKV estimation. On the other hand the sEKV input-referred flicker noise estimation is right on top of PSP. The extracted sEKV flicker noise parameters are given in Table 5.3.

Table 5.3: Extraction of the sEKV flicker noise parameters.

Transistor	W_{eff} $[\mu m]$	L_{eff} $[nm]$	IC [-]	KF $[J]$	AF [-]	ρ_n $\left[\frac{V\,m^2}{A\,s}\right]$	Comment
Mn	10.020	0	0.699	5.837e-25	1.000	2.285e-03	moderate

6 Conclusion

This notebook presented different approaches to extract the sEKV parameters for a short-channel nMOS transistor for the 130nm IHP BiCMOS technology. The data was first obtained by simulations using the PSP compact model and the IHP PDK.

The sEKV parameters were first extracted using a direct extraction methodology with $\lambda_c = 0$. This results in a good fit over all regions of operation except in very strong inversion because of the combined effects of velocity saturation and mobility reduction due to the vertical field.

The direct extraction approach is then used to also extract the velocity saturation parameter λ_c. After some some tuning we can get a very good fit in all regions of operation including strong inversion.

The sEKV parameters are then extracted using curve fitting which immediately gives a good result in all regions of operation with values that are close to those extractied with the direct extraction methodology.

The parameters for the output conductance due to CLM are then extracted in moderate inversion.

Finally, we also have checked that the thermal noise of EKV matches the PSP model and we have extracted the flicker noise parameters.

Overall we have shown that sEKV can fit the large- and small-signal data very well and that the noise is consistent with PSP for this short-channel nMOS transistor.

References

[1] C. C. Enz and E. A. Vittoz, *Charge-Based MOS Transistor Modeling - The EKV Model for Low-Power and RF IC Design*, 1st ed. John Wiley, 2006.

[2] C. Enz, F. Chicco, and A. Pezzotta, "Nanoscale MOSFET Modeling: Part 1: The Simplified EKV Model for the Design of Low-Power Analog Circuits," *IEEE Solid-State Circuits Magazine*, vol. 9, no. 3, pp. 26–35, 2017.

[3] IHP, "IHP SG13G2 Open Source PDK." https://github.com/IHP-GmbH/IHP-Open-PDK, 2025.

[4] G.D.J. Smit, A.J. Scholten, D.B.M. Klaassen, O. Rozeau, S. Martinie, T. Poiroux and J.C. Barbé, "PSP 103.6 - The PSP model is a joint development of CEA-Leti and NXP Semiconductors." https://www.cea.fr/cea-tech/leti/pspsupport/Documents/psp103p6_summary.pdf, 2017.

[5] Han, H.-C. and A. D'Amico and C. Enz, "SEKV-E: Parameter Extractor of Simplified EKV I-V model for Low-power Analog Circuits." https://gitlab.com/moscm/sekv-e, 2022.

[6] H.-C. Han, A. D'Amico, and C. Enz, "SEKV-E: Parameter Extractor of Simplified EKV I-V Model for Low-Power Analog Circuits," *IEEE Open Journal of Circuits and Systems*, vol. 3, pp. 162–167, 2022.

[7] M. Bucher, C. Lallement, C. Enz, F. Theodoloz, and F. Krummenacher, "The EPFL-EKV MOSFET Model Equations for Simulation." https://github.com/chrisenz/EKV/blob/main/EKV2.6/docs/ekv_v26_rev2.pdf, 1998.